# Installation angle offset compensation of puncture robot based on measurement of needle by CT equipment

Akisato Nagao

OKK Corporation,
Hyogo, 664-0831, Japan
Email: pxn81vhp@s.okayama-u.ac.jp

Takayuki Matsuno*

Graduate School of Natural Science and Technology,
Okayama University,
Okayama, 700-8530, Japan
Fax: +81-86-251-8234
Email: matsuno@cc.okayama-u.ac.jp
*Corresponding author

Tetsushi Kamegawa

Graduate School of Interdisciplinary Science
and Engineering in Health Systems,
Okayama University,
Okayama, 700-8530, Japan
Fax: +81-86-251-8023
Email: kamegawa@okayama-u.ac.jp

Takao Hiraki

Graduate School of Medicine,
Dentistry and Pharmaceutical Sciences,
Okayama University,
Okayama, 700-8558, Japan
Email: takaoh@tc4.so-net.ne.jp

**Abstract:** A medical procedure called interventional radiology (IR) is paid much attention in recent years. IR can be performed percutaneously while a doctor observes patient's fluoroscopic image. Therefore this surgical method is low-invasiveness method. In this surgery, computed tomography (CT) equipment is often used. But a doctor is exposed to strong radiation from CT. Thus, we have developed a remote-controlled surgery support robot called 'Zerobot'. Because Zerobot is placed in front of CT equipment by human, an angle offset from installation target position occurs. If a doctor punctures without noticing that Zerobot has an installation angle offset, there is danger of hurting the part that should not be hurt around a target cancer. In order to solve this problem, we propose the installation angle offset derivation method using a CT equipment and an angle offset compensation method is proposed. Then, effectiveness of proposed method is confirmed through experiments.

**Keywords:** surgery support robot; interventional radiology; puncture robot.

**Reference** to this paper should be made as follows: Nagao, A., Matsuno, T., Kamegawa, T. and Hiraki, T. (2018) 'Installation angle offset compensation of puncture robot based on measurement of needle by CT equipment', *Int. J. Mechatronics and Automation*, Vol. 6, No. 4, pp.190–200.

**Biographical notes:** Akisato Nagao graduated Graduate School of Natural Science and Technology in Okayama University, and is currently in OKK corporation. His research interests include medical robot.

Takayuki Matsuno received his Dr. Eng from Nagoya University in 2005, and is in Okayama University. His research interests include manipulation and a robotic manipulator.

Tetsushi Kamegawa received his PhD in Engineering from Tokyo Institute of Technology in 2004, and currently in Okayama University. His research interests include a snake robot and a rescue robot.

Takao Hiraki received his MD from Okayama University in 2001, and currently in Graduate School of Medicine, Dentistry and Pharmaceutical Sciences Okayama University. His research interests include interventional radiology.

This paper is a revised and expanded version of a paper entitled 'Installation angle offset compensation of puncture robot based on measurement of needle by CT equipment' presented at *2017 IEEE International Conference on Mechatronics and Automation (ICMA)*, Takamatsu, Japan, 6 August, 2017.

## 1 Introduction

There is a surgical method called interventional radiology (IR). This surgical method is conducted with imaging modality such as CT and X-rays. With observing medical images, the doctor conducts IR treatment percutaneously with inserting a needle or a catheter to the patient body. In particular, CT equipment has high visibility and objectivity. And CT fluoroscopy system, which can show medical images in real time, is superior as guiding tool for IR. So CT-guided IR is applied to lung cancer treatment, liver cancer treatment, biopsy, and so on (Hiraki et al., 2014). The appearance of manual IR treatment is shown in Figure 1. As compared with conventional survey, IR can be conducted in local anesthesia and this surgical method is minimally-invasive to patients. Moreover patients can be discharged from the hospital about three or four days after treatment. Because of these advantages, IR is paid much attention in recent years. However, IR has disadvantage too. According to the opinion of a doctor, the minimum size of cancer is 5 [mm]. Therefore an doctor must puncture a needle carefully and accurately. In addition, doctors are exposed to radiation during CT fluoroscopy because doctors conduct procedure close to the CT gantry.

**Figure 1** Interventional radiology (see online version for colours)

In order to prevent radiation exposure, doctors wear radiation protection aprons and handle a needle using a forceps which is useful to make distance between hand and CT measure plane. However, it is impossible to prevent radiation exposure completely. Then some medical robots are developed in order to improve accuracy of positioning of a needle, and to reduce radiation exposure, such as AcuBot (Staianovici et al., 2003), CT-Bot (Maurin et al., 2008) and MAXIO (Koethe et al., 2013). These robots aim to support doctors to insert a needle as CT-guided puncture. However, Zerobot, which is developed by our research group, aims to conduct whole process from positioning robot to inserting a needle by remote-control.

In this research, in order to seek the problem of Robotic IR system, we have conducted phantom puncture experiment (Nakaya et al., 2014) and animal puncture experiment (Sugiyama et al., 2015). In addition, risk management is conducted. Since Zerobot is used for medical purposes, Zerobot must be safe. Safety of Zerobot is confirmed by a lot of nonclinical studies which are part of risk management. But some problems are confirmed too. These problems make time of surgery longer and increasing patient exposure to accurately puncture. Zerobot is remotely operated far from CT equipment by a doctor with using a control device. Since Zerobot held a needle at surgery, the doctor must carefully operates Zerobot so that tip of needle could not touch patient on bed. Therefore, much time is needed to target a needle. The doctor should pay attention in order to bring the needle to feasible pose without accident of collision. In addition, CT plane position is not shown accurately by a laser light which shows CT plane position. Therefore, CT scanning is conducted after the targeting. If a needle is not shown in CT image, targeting and scanning will be retried. Since, the patient is not guard from exposure in this time, the risk occurs that the patient is exposed more than necessary. Therefore, we implemented the automatically registration and targeting function in previous research.

Firstly, a doctor specifies the current needle tip position and the canner position with the CT equipment. Secondly, a computer calculates displacement of each axis to make the needle tip pose before puncturing. The doctor operates the Zerobot by NC operation based on this calculation result. This function reduces CT scan time and reduces patient exposure. However, this function does not consider influence an installation angle offset of Zerobot. Therefore, if Zerobot is not installed parallel to the CT equipment, it is impossible to bring the needle tip to the target pose correctly. Because Zerobot is installed onto floor of surgical room by human, an angle offset around vertical axis from installation target position occurs as shown in Figure 2. If a doctor punctures without noticing that Zerobot has the installation angle offset, Zerobot will be puncture a position that is not target. It will be bring medical accident. Therefore, we propose a method to compensate installation angle offset between Zerobot and CT equipment.

**Figure 2** Zerobot setting position (see online version for colours)

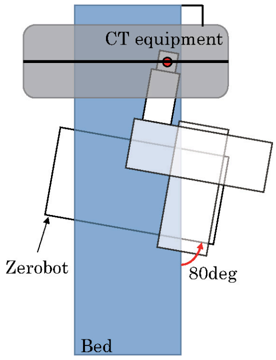


## 2 Specifications

### 2.1 Workspace

Zerobot has to handle a needle within cylindrical space of CT gantry in order to make the needle direction to target tumour. The diameter of the inside of a gantry is small. When a patient lies on a bed, the space becomes smaller. Therefore, the work space to handle a needle is very narrow. The dimensions of work space are shown in Figure 4. The inner diameter of the gantry is 720 mm. The width of a bed on which a patient lies is 450 mm and the thickness is 50 mm. We assume that the width of a patient is 500 mm and the thickness is about 150–200 mm. Moreover, the point to start to puncture varies depending on a position of affected part and the location of bones of a patient. It is necessary for the robot to set a needle to any position and orientation where previously planned based on CT image. Then the robot starts puncturing. According to the opinion of a medical doctor, a needle has to be tilted $\pm 20$ degrees around craniocaudal direction and $\pm 90$ degrees around circumferential direction in maximum. In order to satisfy the requirement, a mechanical design to achieve wide orientation in a small work space is required.

### 2.2 Degree of freedom

Zerobot has six degrees of freedom (DOF) in order to locate an end effector in any position and orientation. In the case of robotic IR system, one degree of freedom is able to be omitted because a degree of freedom around an axis of a needle is not required. Therefore the robot has to have five DOF at least. In addition, according to a procedure of IR, a needle moves almost straight after determining the initial pose of insertion. It is desirable to achieve straight motion by using only one actuator when the robot achieves puncturing motion in order to realise high accuracy.

### 2.3 Artifacts

Artifacts are also an issue to realise a CT-guided puncturing robot. Artifacts are kinds of noise which appear on CT images with black or white shadow. The noise is caused metal materials in a gantry of CT equipment because metal parts absorbs X-ray. Generally, this kind of artifacts tend to occur in the case that X-ray absorption rate of material is high and the X-ray transmittance distance is significantly different according to measuring direction (Monkawa, 2012).

If artifacts overlap onto the target tumour in the CT image, it makes an doctor difficult to understand the position of tumour property and to achieve precise operation. To avoid this problem, a CT-guided puncturing robot is not able to use metal parts in its end effector, especially the parts where have possibility to be scanned by CT machine. Note that a needle has metal part and it generates artifacts. However, this artifacts is allowed and utilised by an doctor as a guideline to puncture to the target in practice because the artifacts indicate the direction of the needle.

## 3 Overview of robotic IR

### 3.1 System structure

This subsection describes the system structure of Zerobot. The system structure of Zerobot is shown in Figure 7. Zerobot is connected to computer of interface device via Ethernet to communicate by TCP/IP. As receiving the information of status of interface device, a computer of interface device instructs to Zerobot to actuate axes. Zerobot sends the angle or displacement of six joints and force sensor to interface devices. In the interface devices, process to command the trajectory of Zerobot and navigation display is divided, and status of Zerobot received by program of controlling Zerobot is sent by shared memory to program of navigation display.

### 3.2 Mechanism

The appearance of Zerobot is shown in Figure 3. It has five DOF for needle tip position and needle direction, and has one DOF for puncturing direction. Six actuators are in the machine. Four linear actuators ($X, Y, Z$ and puncturing axes directions) and two rotational actuators (around the $X$ and $Y$ axes) are included.

Therefore, Zerobot can perform puncture operation by actuating the puncturing axis, regardless of the posture. Four passive wheels are mounted on the bottom of the robot, so that it can be moved with human power. At the surgical operation, the robot is located under a bed and fixed by locking the wheels (Figure 5). Changing needle direction and puncturing are performed in CT-gantry by arm part above patient.

Accordingly parts are made of engineering plastic, which is radiolucent material. Motor for puncture is required in end-effector. The angle of elevation of CT equipment can be changed as necessary, as shown in Figure 6.

### 3.3 Procedure of puncture

This subsection describes procedure of Robotic IR. The procedure is listed as below.

- *Scanning whole abdomen*

  Target tumour's position is confirmed from patient's CT image.

**Figure 3** Appearance of Zerobot (see online version for colours)

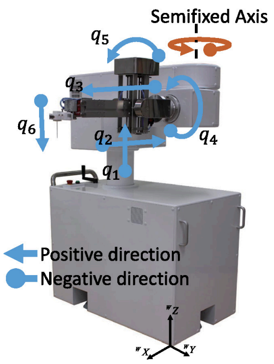


**Figure 4** Work space for a CT-guided puncturing robot (see online version for colours)

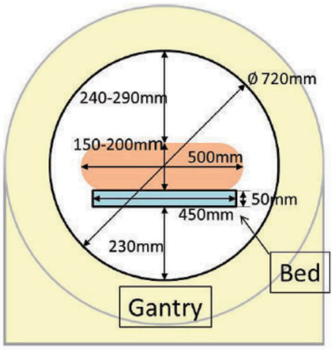


**Figure 5** Reproduction of surgical environment (see online version for colours)

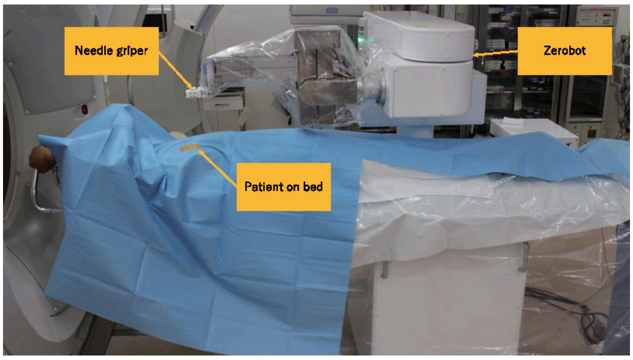


- *Planning*

  Relation between catheter marker and tumour position is confirmed by CT image, and puncture path is planned. Then, a puncturing point on surface of skin is marked by pen.

- *Adjustment of needle tip pose*

  Needle is brought to CT radiography plane based on laser emitted from CT equipment. And needle tip position is adjusted to marked position on surface of skin. Then, needle direction is also adjusted to preplanned angle.

- *Fine adjustment of needle direction*

  Needle direction is made fine adjustments so as to direct a needle to the target tumour, under CT fluoroscopic guidance. Artifact from needle can be regarded as extension line of needle.

- *Puncture*

  Needle is punctured into body. When the depth of puncture reaches the preplanned value, the doctor confirms relation between position of needle tip and centre of tumour by observing CT radiography. And then, either needle tip position or needle direction is readjusted as necessary.

Zerobot is used in abovementioned sequence. If robot cannot manipulate needle accurately, the doctor have to readjust the posture of needle based on real time CT image. It increases patient's radiation exposure. Therefore, accuracy of robot hand position is required.

**Figure 6** Definition of CT radiography plane (see online version for colours)

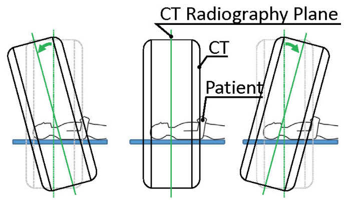


**Figure 7** System structure of robotic IR (see online version for colours)

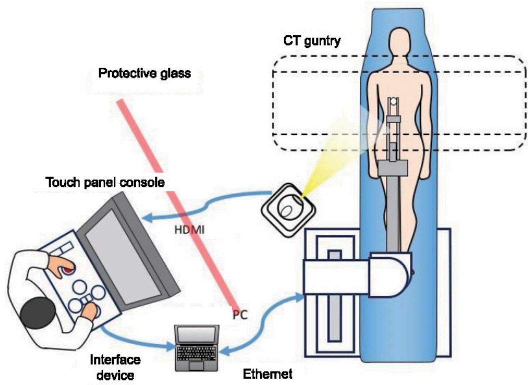


### 3.4 Interface system

Design of interface device is important to safe operation because Zerobot is remotely operated by a doctor. Developed interface device is shown in Figure 8. This interface consists from a touch panel display and master controller. State observation and mode switching can be done on the touch panel display. Zerobot is basically operated with master controller. Motion correspondence diagram of master controller is shown in Figure 9. $X$, $Y$ and $Z$ mean same as $q_2$, $q_1$ and $q_3$ in Figure 3. Rocker switch for Z axis has three states. Zerobot is operated to positive direction of $q_3$ when upper side is pushed. On the other hands, Zerobot is operated to negative direction of $q_3$ when lower side is pushed. Zerobot is operated to rotate axis with cross key. Motion around A axis is operated with left and right keys. Motion around B axis is operated with upper and lower keys. Servo state is changed with centre button in cross key. Puncture axis is operated with left side rocker switch. The needle is punctured when lower side is pushed. On the other hands, the needle is withdrawn when upper side is pushed. These axis can be driven by certain button with pushing ‘slow’ or ‘fast’ button simultaneously for safety reasons. Risk of unintentional operating is decreased by this function. In addition, puncture axis can be operated only when puncture mode is validity because risk of damage patient is higher when puncture axis is operated. Puncture mode can be changed on touch panel display. Left upper side covered button is used for ultra fast puncture with air actuator. The air actuator drawbacks when left upper side uncovered button is pushed.

**Figure 8** Configuration of control unit: (a) appearance control unit; (b) touch panel display and (c) master controller (see online version for colours)

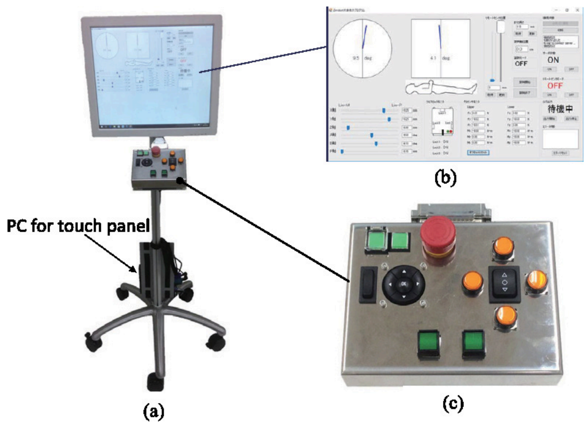


**Figure 9** Correspondence of master controller (see online version for colours)

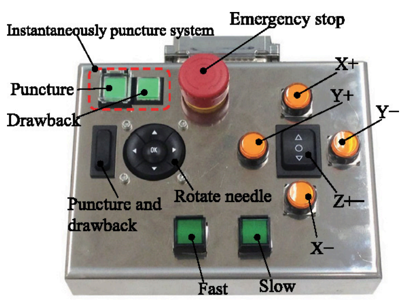


## 3.5 *Risk management*

Risk management is conducted for clinical trial. Since Zerobot is used for medical purposes, Zerobot must be safe. Therefore, risk management should be conducted. In previous research, nonclinical study as part of risk management was conducted. In nonclinical study, equivalent verification test of puncture performance for compared with hand operation was conducted with phantom. It was confirmed that Zerobot can puncture a needle as correctly as doctor’s hands by equivalent verification test. Animal simulation test is also conducted in nonclinical study too. It was confirmed that Zerobot can puncture a needle into living tissue by animal use simulation test. A number of other nonclinical studies were conducted to confirm that Zerobot can be used safety. (Hiraki et al., 2017)

## 3.6 *Problems for clinical trial*

In conducted risk management, it turned out that there were problems with needle puncture with Zerobot. CT scanning is conducted after the targeting. If a needle is not shown in CT image, targeting and scanning will be retried. Since, the patient is not guard from exposure in this time, the risk is occurred that the patient is exposed more than necessary. This problem cause is that the registration is not done before targeting. It is called registration that CT plane position and needle position are defined same coordinate system. If registration method is developed, the patient will be not exposed more than necessary. Therefore, Automated registration and targeting function is proposed in previous research.

# 4 Automatically registration and targeting

Automated registration and targeting function are described in this section. Outline of sequence is shown in Figure 10. Firstly, a needle which griped by Zerobot and target in patient body are scanned with CT equipment. Needle tip position and target position are defined in robot base coordinate system($\Sigma_0$) based on CT scanning data. This procedure is called automatically registration.

**Figure 10** System of automatic registration and targeting (see online version for colours)

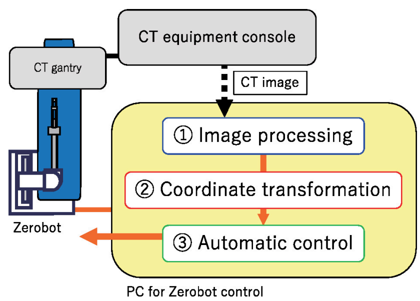


Secondly, CT scanning data is sent to an image processing software. Target needle pose is decided in image processing software by the doctor. Initial position of robot to puncture a needle into body is automatically calculated according to relation between current needle position and target needle pose. Initial joint angles of Zerobot is calculated from initial position of robot to puncture a needle into body by inverse kinematics. Zerobot is operated by NC operation based on this calculation result. This procedure is called automatically targeting.

These function consists image processing software, coordinate conversion software and Automatic control software. These software are described following subsections.

## 4.1 *Image processing software*

After installing Zerobot, firstly, a needle held by Zerobot is scanned with CT equipment when using this software.

Zerobot should be installed where needle can be scanned in this procedure. Secondly, target in patient body is scanned with CT equipment.

After scanning a needle and target, CT images are sent to image processing software. In this software, Actual needle tip position is marked on CT image by the doctor. Actual needle tip position in $\Sigma_0$ is automatically calculated. Since, Zerobot take an initial pose in this procedure, the needle posture is $\phi_A = 0.0$[deg] and $\phi_B = 0.0$[deg]. Then, a target position and a puncturing point are marked by doctor. The target position to the puncturing point line is a puncture route. Vital organs, for example, bone and artery, must not exist on the puncture route. Since, avoiding the needle hurting the patient's body when Zerobot is automatically operated, the puncturing point should be distant about 10[mm] from patient's body. The puncture position and a posture of puncture route are automatically converted to pose in CT coordinate system. Actual needle pose and target needle pose are defined in $\Sigma_0$ with these procedure. Therefore, it can be said that automatic Registration is finished. Finally, initial position of robot to puncture a needle into body is automatically calculated according to relation between actual needle pose and target needle pose.

## 4.2 *Coordinate conversion software*

Initial position of robot to puncture a needle into body is converted to initial joint angles of Zerobot by inverse kinematics. Therefore, kinematics analysis is described in this subsection.

Zerobot has six active joints and a semifixed joint as shown in Figure 3. Each axis' positive direction is represented by arrows. Semifixed axis is fixed to -90[deg] or 90[deg] as shown in Figure 11(b). Six active axes' angles[deg] or displacements[mm] are defined as $\boldsymbol{q} = [q_1, q_2, \ldots, q_6]^T$. $q_1, q_2, q_3$ and $q_6$ are linear axes, and $q_4$ and $q_5$ are rotation axes. And needle tip position and needle posture are defined as ${}^0\boldsymbol{r}_E = [x, y, z, \phi_A, \phi_B]^T$. $\phi_A$ and $\phi_B$ are defined as Figure 11(a). $\phi_A$ is the angle of needle on the CT radiography plane, and $\phi_B$ is the gantry tilt angle of the plane. Since the needle is line symmetric, five variables ignoring the rotation around the centre axis of the needle are output. Forward kinematics is projection of vector from $\boldsymbol{q}$ to ${}^0\mathbf{r_E}$, and inverse kinematics is projection of vector from ${}^0\boldsymbol{r}_E$ to $\boldsymbol{q}$. Hereafter, $\sin\theta$ is represented as $S_\theta$, and $\cos\theta$ is represented as $C_\theta$. In addition, there is one thing that should be noted here. Originally, in the all of equations for kinematics elements of $C_{\alpha_3}$ should be included (Definition of $\alpha_3$ is described in after this subsection.). But $\alpha_3$ can only take the value of 90[deg] or –90[deg]. In this case, the value of $C_{\alpha_3}$ must be zero. Therefore, elements of $C_{\alpha_3}$ are omitted from all of equations for kinematics in this paper.

### 4.2.1 *Forward kinematics*

Forward kinematics of Zerobot is derived by Denavit-Hartenberg notation (DH notation) (Craig, 1989). Location of coordinate systems is listed in Figure 12. These coordinate systems are located following DH notation. DH parameters are shown in Table 1. In the table, the value of $\alpha_3$ depends on semifixed axis direction. And definition of required parameters $l_1$, $l_2$ and $l_3$ is also shown in Figure 12. So we can calculate ${}^0\boldsymbol{T}_6$, which is homogeneous transformation matrix from $\Sigma_0$ to $\Sigma_6$. And ${}^6\boldsymbol{T}_E$ is just translate transformation depending on needle length defined as $l_E$. Therefore, ${}^0\boldsymbol{T}_E$ can be calculated as follows.

$$ {}^0\boldsymbol{T}_E = \begin{bmatrix} -S_{q_4}S_{q_5}S_{\alpha_3} & C_{q_4}S_{\alpha_3} & S_{q_4}C_{q_5}S_{\alpha_3} & {}^0r_{Ex} \\ C_{q_5}S_{\alpha_3} & 0 & S_{q_5}S_{\alpha_3} & {}^0r_{Ey} \\ C_{q_4}S_{q_5} & S_{q_4} & -C_{q_4}C_{q_5} & {}^0r_{Ez} \\ 0 & 0 & 0 & 1 \end{bmatrix}, \quad (1) $$

$$ \begin{aligned} {}^0r_{Ex} &= l_3 - q_3 + l_2 S_{q_4}S_{\alpha_3} + (q_6 + l_9 + l_E)S_{q_4}C_{q_5}S_{\alpha_3} \\ &\quad + l_7 S_{q_4}S_{q_5}S_{\alpha_3}, \\ {}^0r_{Ey} &= (q_6 + l_9 + l_E)S_{q_5}S_{\alpha_3} + q_2 - l_1 S_{\alpha_3} + l_7 C_{q_5}S_{\alpha_3}, \\ {}^0r_{Ez} &= q_1 - l_2 C_{q_4} - (q_6 + l_9 + l_E)C_{q_4}C_{q_5} - l_7 C_{q_4}C_{q_5}. \end{aligned} $$

**Table 1** DH parameters

| i | $\alpha_{i-1}$ | $a_{i-1}$ | $d_i$ | $\theta_i$ |
|---|---|---|---|---|
| 1 | 0 | 0 | $q_1$ | 0 |
| 2 | –90 | 0 | $q_2$ | –90 |
| 3 | 90 | 0 | $q_3 - l_3$ | 0 |
| 4 | 90 or –90 | 0 | $l_1$ | $180 + q_4$ |
| 5 | –90 | $l_2$ | 0 | $90 + q_5$ |
| 6 | 90 | 0 | $q_6$ | 0 |

**Figure 11** Important parameters in the kinematics: (a) definition of $\phi_A$ and $\phi_B$ and (b) states image which can be taken by semifixed axis (see online version for colours)

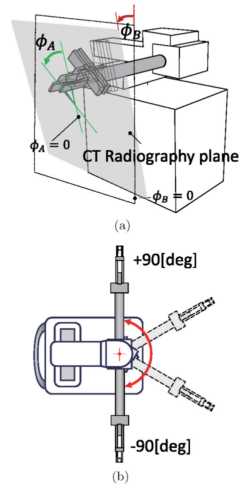


Next, $\phi_A$ and $\phi_B$ corresponding to needle posture should be calculated. Then, direction vector of needle represented on $\Sigma_0$ is defined as ${}^0\boldsymbol{n}_E$. ${}^0\boldsymbol{n}_E$ equals third column direction vector of rotation matrix of ${}^0\boldsymbol{T}_E$. Therefore ${}^0\boldsymbol{n}_E$ is represented as (2).

$$ {}^0\boldsymbol{n}_E = \begin{bmatrix} S_{q_4}C_{q_5}S_{\alpha_3} & S_{q_5}S_{\alpha_3} & -C_{q_4}C_{q_5} \end{bmatrix}^T. \quad (2) $$

Here, ${}^0\boldsymbol{n}_E$ also can be represented with $\phi_A$ and $\phi_B$ as follow. When we make the rotation matrix including $\phi_A$ and $\phi_B$ which

**Figure 12** Location of coordinate systems. Coordinate systems which are looking from side is shown in (a). Coordinate systems which are looking from front is shown in (b). Coordinate systems around end-effector is shown in (c): (a) side view; (b) front view and (c) end-effector (see online version for colours)

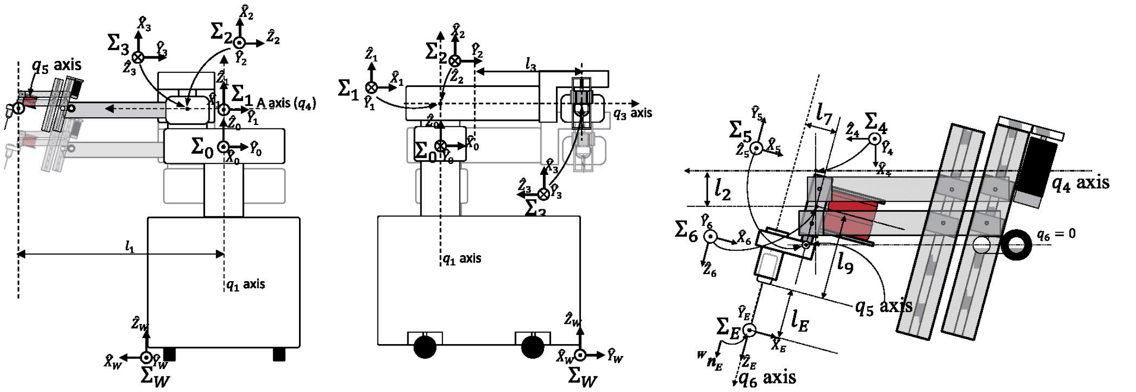


(a) (b) (c)

can coincide direction of z axis of $\Sigma_0$ with $\hat{Z}_E$ direction, third column direction vector of the rotation matrix is ${}^0\boldsymbol{n}_E$.

$$
\begin{aligned}
{}^0\boldsymbol{n}_E &= \boldsymbol{R}_{\boldsymbol{x}(-\pi/2)}\boldsymbol{R}_{\boldsymbol{z}(\alpha_3)}\boldsymbol{R}_{\boldsymbol{x}(\phi_B)}\boldsymbol{R}_{\boldsymbol{y}(\phi_A)}\begin{bmatrix}0\\0\\1\end{bmatrix} \\
&= \begin{bmatrix} S_{\alpha_3}S_{\phi_A} \\ S_{\alpha_3}C_{\phi_A}S_{\phi_B} \\ -C_{\phi_A}C_{\phi_B} \end{bmatrix}.
\end{aligned} \tag{3}
$$

As comparing between (2) and (3), $\phi_A$ and $\phi_B$ can be calculated as (4), (5).

$$\phi_B = \tan^{-1}\left(\frac{1}{C_{q_4}}\tan q_5\right), \tag{4}$$

$$\phi_A = \tan^{-1}\left(C_{\phi_B}\tan q_4\right). \tag{5}$$

Finally, ${}^0\boldsymbol{r}_E$ is calculated as (6).

$$
{}^0\boldsymbol{r}_E = \begin{bmatrix}
l_3 - q_3 + l_2S_{q_4}S_{\alpha_3} + q_6S_{q_4}C_{q_5}S_{\alpha_3} + l_ES_{q_4}C_{q_5}S_{\alpha_3} \\
q_6S_{q_5}S_{\alpha_3} + q_2 - l_1S_{\alpha_3} + l_ES_{q_5}S_{\alpha_3} \\
q_1 - l_2C_{q_4} - q_6C_{q_4}C_{q_5} - l_EC_{q_4}C_{q_5} \\
\tan^{-1}\left(C_{\phi_B}\tan q_4\right) \\
\tan^{-1}\left(\frac{1}{C_{q_4}}\tan q_5\right)
\end{bmatrix}. \tag{6}
$$

### 4.2.2 Inverse kinematics

In this section, procedure of inverse kinematics is described. Target needle tip position is defined as ${}^0\boldsymbol{r}_E^* = [x^*, y^*, z^*, \phi_A^*, \phi_B^*]^T$. And target robot posture is defined as $\boldsymbol{q}^* = [q_1^*, q_2^*, \ldots, q_6^*]^T$. According to (6), relationship between $\boldsymbol{q}^*$ and ${}^0\boldsymbol{r}_E^*$ is represented as follows.

$$x^* = (l_E + q_6)\,S_{q_4^*}C_{q_5^*}S_{\alpha_3} + l_2S_{q_4^*}S_{\alpha_3} + l_3 - q_3^*, \tag{7}$$

$$y^* = (l_E + q_6)\,S_{q_5^*}S_{\alpha_3} - l_1S_{\alpha_3} + q_2^*, \tag{8}$$

$$z^* = q_1^* - l_2C_{q_4^*} - (l_E + q_6)\,C_{q_4^*}C_{q_5^*}, \tag{9}$$

$$\phi_B^* = \tan^{-1}\left(\frac{1}{C_{q_4^*}}\tan q_5^*\right), \tag{10}$$

$$\phi_A^* = \tan^{-1}\left(C_{\phi_B^*}\tan q_4^*\right). \tag{11}$$

Inverse kinematics can be derived from equation (7) to equation (11). But Zerobot has redundant DOF. Therefore we derived inverse kinematics in under the assumption that $q_6$, which is puncture axis, is fixed and is known. Then, inverse kinematics is derived as follows.

$$q_4^* = \tan^{-1}\left(\frac{1}{C_{\phi_A^*}}\tan\phi_B^*\right), \tag{12}$$

$$q_5^* = \tan^{-1}\left(C_{q_4^*}\tan\phi_A^*\right), \tag{13}$$

$$q_1^* = z^* + l_2C_{q_4^*} + (l_E + q_6)\,C_{q_4^*}C_{q_5^*}, \tag{14}$$

$$q_2^* = l_1S_{\alpha_3} - (l_E + q_6)\,S_{q_5^*}S_{\alpha_3} + y^*, \tag{15}$$

$$q_3^* = l_2S_{q_4^*}S_{\alpha_3} + (l_E + q_6)\,S_{q_4^*}C_{q_5^*}S_{\alpha_3} + l_3 - x^*. \tag{16}$$

## 4.3 Automatic control software

Zerobot is operated by NC operation based on the previous subsection calculation result with this software. Zerobot is controlled by PI control according to relation between each axis angle value and target value(Figure 13). When all axis arriving initial position, automatic targeting is complete. After the automatic targeting, conventional robotic IR procedure is conducted by doctor.

**Figure 13** Control system of robot (see online version for colours)

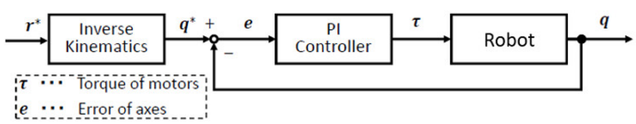


## 4.4 Effect of automatically registration and targeting

In previous research, automated registration and targeting experiment is done with phantom for medical image. Firstly, targeting time is compared. Average targeting time when Zerobot is operated without automatically registration and targeting function is 78[s]. On the other hands, average targeting time when Zerobot is operated with automatically registration and targeting function is 6[s]. The targeting time is less than one-tenth when using automatically registration and targeting function. Since, average targeting time when targeting by the doctor hands is 21[s], it can be seen that automatically registration and targeting function has advantage in time. Secondly, average patient exposed value is compared. Average patient exposed value when Zerobot is operated without automated registration and targeting function is 58[uSv]. On the other hands, average patient exposed value when Zerobot is operated with automatically registration and targeting function is 0[uSv]. In addition, average patient exposed value when targeting by the doctor hands is 58[uSv]. Therefore, it can be seen that automated registration and targeting function has also advantage in minimally exposure too. We found the tendency that position error after conducting automated registration and targeting function became larger under the condition initial position is farther from targeting position.

### *4.5 Problem of automatically targeting function*

In coordinate conversion software, kinematics is calculated in disregard of installation angle offset. Therefore, if Zerobot is not installed parallel to the CT equipment, it is impossible to bring the needle tip to the target pose correctly. Since Zerobot is installed into floor of surgical room by human, an angle offset around vertical axis from optimal position occurs. Zerobot cannot be installed without installation angle offset. Therefore, we proposed installation angle offset compensation method.

## 5 Installation angle offset compensation method

### *5.1 Coordinate systems*

Zerobot base coordinate system is defined as Figure 3. In addition, since CT images are used for our experiment, a coordinate system of the CT image should be defined as Figure 14. Vertical line, horizontal line and depth line mean $X_{CT}$,$Y_{CT}$,$Z_{CT}$. The pixel size of CT in this paper is fixed as 0.8 [mm/pixel]. A coordinate system of the doctor's point of view is also defined as Figure 15. $\Sigma_D$ is optimal position of $\Sigma_W$. Therefore, if Zerobot is installed ideal position, $\Sigma_W$ is same as $\Sigma_D$.

$X_{CT}$ and $Y_D$ have opposite direction each other, on the other hands, $Z_{CT}$ and $X_D$ have same direction.

### *5.2 Method of estimate the installation angle offset of Zerobot*

In order to compensate installation angle offset of Zerobot, it is necessary to estimate the installation angle offset. After installing Zerobot to the position as shown in Figure 5, first the $z_{CT}$ position of the needle with CT equipment is measured. Secondly, Zerobot is operated to move along with $y_W$ direction by 20 mm and the $z_{CT}$ position of the needle is measured. This procedure is repeated until the $y_W$ arrives 200 mm. A first order approximation equation is obtained using the least squares method.

$$z_{CT} = a\,y_W + b \tag{17}$$

The relationship between a centre position of needle tip centre and an angle offset of Zerobot can be obtained a following equation according to Figure 16.

$$\theta_r = -\sin^{-1}\left(\frac{\Delta z_{CT}}{\Delta y_W}\right). \tag{18}$$

Experiments to measure the robot installation angle offset is described later.

**Figure 14** CT coordinate system (see online version for colours)

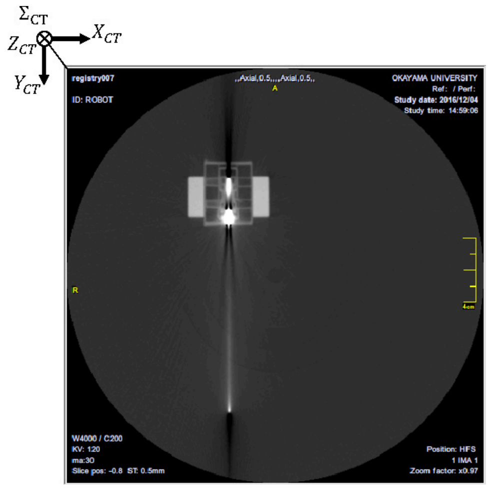


**Figure 15** Doctor coordinate system (see online version for colours)

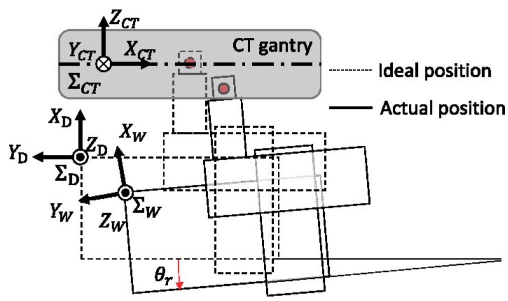


**Figure 16** Derivation of angle offset (see online version for colours)

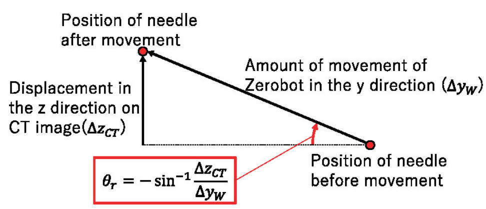


### *5.3 Calculation of target value*

In this subsection, the method to compensate a motion of robot based on Zerobot installation angle offset is described. A needle tip target pose $\left[{}^D x_E^*, {}^D y_E^*, {}^D z_E^*, {}^D \phi_A^*, {}^D \phi_B^*\right]$ in coordinate system $\Sigma_D$ is converted into target pose in coordinate system $\Sigma_W$. The doctor viewpoint coordinate system $(\Sigma_D)$ is converted to the coordinate system of the robot viewpoint $(\Sigma_W)$ by the following rotation matrix.

$$
\begin{aligned}
{}^W\boldsymbol{T}_D &= \begin{bmatrix} \cos\theta_r & -\sin\theta_r & 0 \\ \sin\theta_r & \cos\theta_r & 0 \\ 0 & 0 & 1 \end{bmatrix}^{-1} \\
&= \begin{bmatrix} \cos\theta_r & \sin\theta_r & 0 \\ -\sin\theta_r & \cos\theta_r & 0 \\ 0 & 0 & 1 \end{bmatrix}.
\end{aligned} \tag{19}
$$

Firstly, a needle tip target position is converted by a following equation.

$$
\begin{aligned}
\begin{bmatrix} x_E^* \\ y_E^* \\ z_E^* \end{bmatrix} &= {}^W\boldsymbol{T}_D \begin{bmatrix} {}^Dx_E^* \\ {}^Dy_E^* \\ {}^Dz_E^* \end{bmatrix} \\
&= \begin{bmatrix} {}^Dx_E^* \cos\theta_r + {}^Dy_E^* \sin\theta_r \\ -{}^Dx_E^* \sin\theta_r + {}^Dy_E^* \cos\theta_r \\ {}^Dz_E^* \end{bmatrix}.
\end{aligned} \tag{20}
$$

Secondly, direction cosine vector is converted by the following equation.

$$
\begin{aligned}
\boldsymbol{n}_E^* &= {}^W\boldsymbol{T}_D {}^D\boldsymbol{n}_E^* \\
&= \begin{bmatrix} S_{\alpha_3} S_{D\phi_A^*} \cos\theta_r + S_{\alpha_3} C_{D\phi_A^*} S_{D\phi_B^*} \sin\theta_r \\ -S_{\alpha_3} S_{D\phi_A^*} \sin\theta_r + S_{\alpha_3} C_{D\phi_A^*} S_{D\phi_B^*} \cos\theta_r \\ -C_{D\phi_A^*} C_{D\phi_B^*} \end{bmatrix}.
\end{aligned} \tag{21}
$$

$\phi_A^*$ and $\phi_B^*$ are calculated using first and second rows of (21).

$$
\phi_A^* = \sin^{-1}\left( S_{D\phi_A^*} \cos\theta_r + C_{D\phi_A^*} S_{D\phi_B^*} \sin\theta_r \right), \tag{22}
$$

$$
\phi_B^* = \sin^{-1}\left( \frac{-S_{D\phi_A^*} \sin\theta_r + C_{D\phi_A^*} S_{D\phi_B^*} \cos\theta_r}{C_{\phi_A^*}} \right). \tag{23}
$$

Values obtained by equations (20), (22) and (23) are substituted into the equations from equations (12) to (16). This method realises functions that a doctor can control Zerobot along with coordinate system $\Sigma_D$ even thought installation angle $\theta_r$ exists.

## 6 Experiment

### *6.1 Estimate the installation angle offset of Zerobot*

In order to compensate an installation angle offset, first the offset is measured by using CT equipment. An experiment procedure to measure the installation angle offset was written in subsection 5.2. Zerobot is installed with approximately –10 [deg] against CT equipment by setting the Zerobot at about 80 [deg] against a side of the bed (Figure 2). The result of the experiment is described below. First of all, the installation angle offset of Zerobot is calculated from the amount of movement of Zerobot $Y_W$ axis and the amount of movement of CT coordinate system in the $z_{CT}$ direction. To measure the position of the needle, images of the needle are extracted from the image group at each operating position. In order to decide needle tip position on $z_{CT}$ direction, a feasible image should be selected manually. In this paper, an image which has the brightest needle is selected to measure needle tip position. However, when the extracted images are an even number, select the image owing a longer needle pare is selected as shown in (Figure 17). When the $Y_W$ axis is 0 [mm], the deviation from each operating position with $Z_{CT}$ as the origin is taken as the movement amount of the needle in the $Z_{CT}$ direction.

**Figure 17** Needle centre position of $Z_{CT}$ direction. In this case, the needle centre position is (c): (a) $Z_{Cr} = 2.0$[mm]; (b) $Z_{Cr} = 2.5$[mm]; (c) $Z_{Cr} = 3.0$[mm] and (d) $Z_{Cr} = 3.5$[mm] (see online version for colours)

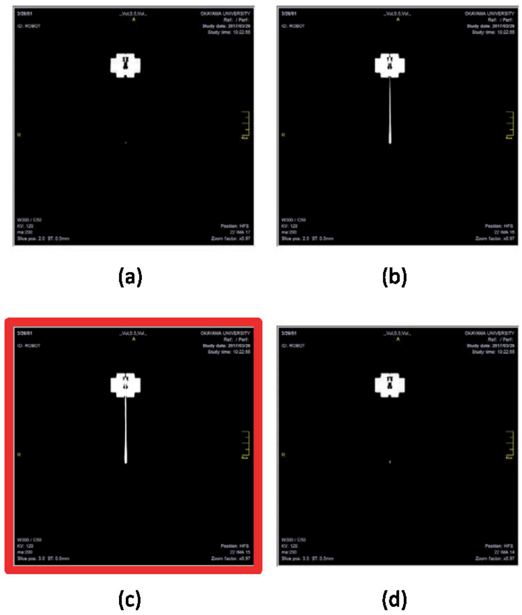


An approximate straight line equation can be calculated as $z_{CT} = 0.175\, y_W$ from Figure 18 . The installation angle offset of Zerobot is calculated as $-10.08$ [deg] from equation (18) and the approximate straight line equation. It is almost equal to the installation angle of Zerobot and it can be said that the measurement is successful.

### *6.2 Installation angle offset compensation*

After estimation of installation angle offset $\theta_r$, desired hand position of robot is calculated according to equations from (21) to (24). First, $\theta_r$ = –10.08 [deg] is set in those equations in order to calculate compensated desired position in this experiment. Next hand position of robot moves in $Y_D$ direction from 0 [mm] to 200 [mm] per 20 [mm]. In each pose, CT scanning is conducted to acquire the position of needle tip so as to obtain deviation in $Y_D$ direction. Amount of $X_D$-axis and $Y_D$-axis direction motions of doctor coordinate system are verified from the taken image. The experiment result is shown in Figure 19. We define an error tolerance in $Y_D$ position to 2.5 [mm] because the minimum diameter of the cancer is 5 [mm]. In the operation without compensation, the centre position of the needle greatly deviates from the tolerance error. However, suppressing the maximum value of error within tolerance is succeed by angle offset compensation control.

**Figure 18** Amount of movement in the $z_{CT}$ direction during Zerobot y-axis operation (see online version for colours)

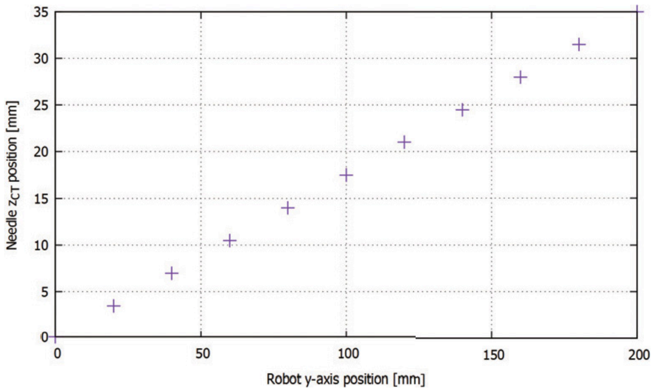


**Figure 19** Needle tip centre position error when moving Zerobot in $Y_D$ direction with an installation angle offset of –10.08 degree (see online version for colours)

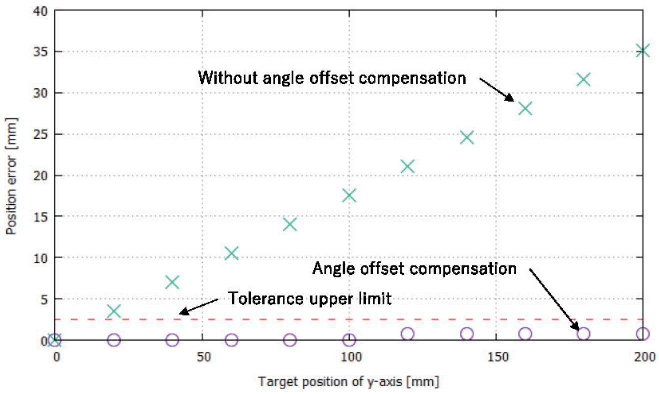


Secondly, the motion accuracy is verified in $X_D$-axis direction. The position of needle is measured each time while the robot moves along $X_D$ direction from 0 [mm] to 100 [mm] per 10 [mm]. Figure 20 shows the error when the robot moves in the $X_D$ direction. When operating the robot in the $X_D$ direction with the angle offset compensation function, the needle tip centre position error cannot be founded. Figures 19 and 20 show that the angle offset compensation controls in the orthogonal direction were successful.

Next, the rotation motion accuracy around $\phi_A$-axis direction is verified. As shown in Figure 21 , the angle error is measured with the inner product of the unit vector of the ideal needle posture $\left[{}^I x_{CT}, {}^I y_{CT}, {}^I z_{CT}\right]$ and the unit vector of the actual needle posture $\left[{}^A x_{CT}, {}^A y_{CT}, {}^A z_{CT}\right]$ as equation (24). Unit vector of the actual needle posture is measured from the deviation of the tip and the root position of the needle based on the CT image.

$$\theta_{\text{error}} = \cos^{-1}\left({}^A x_{CT}{}^I x_{CT} + {}^A y_{CT}{}^I y_{CT} + {}^A z_{CT}{}^I z_{CT}\right) \tag{24}$$

Tolerance of the angle is set to 1.43 [deg] or less. Because the needle tip deviation should be suppressed within 2.5 [mm] when puncturing 100 [mm],

$$\Delta\phi_A^{\max} = \sin^{-1}\left(\frac{2.5}{100}\right) = 1.43\,[\text{deg}] \tag{25}$$

The posture of needle is measured each time while the robot rotates around $\phi_A$ direction from -80 [deg] to 80 [deg] per 10 [deg]. Figure 22 shows error of angle $\phi_A$. In the operation without compensation, the posture of needle also greatly deviates from the tolerance error. Same as position, posture error can also be adjusted to the allowable error by angle offset compensation.

**Figure 20** Needle tip centre position error when moving Zerobot in $X_D$ direction with an installation angle offset of –10.08 degree (see online version for colours)

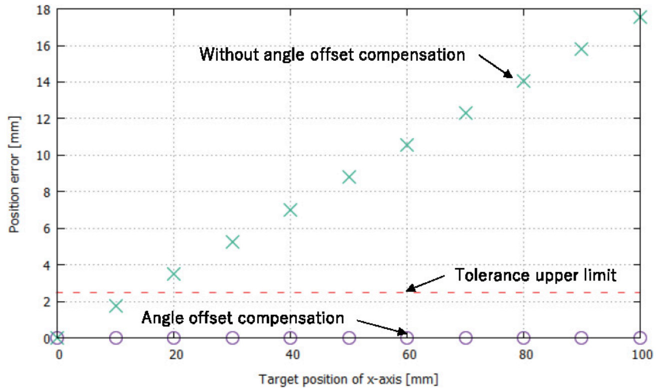


**Figure 21** Measurement method of angle error (see online version for colours)

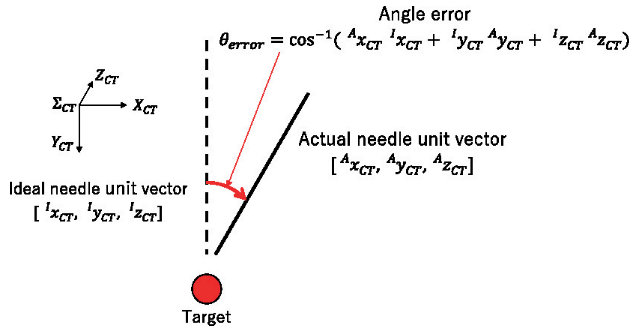


**Figure 22** Needle posture error when rotating hand of Zerobot around $\phi_A$ direction with an installation angle offset of –10.08 degree (see online version for colours)

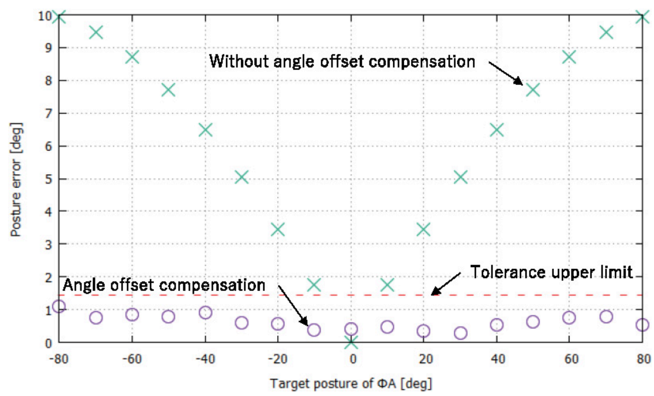


Finally, the motion accuracy around $\phi_B$-axis direction is verified. The posture of needle is measured each time while the robot rotates around $\phi_B$ direction from –10 [deg] to 10

[deg] per 2 [deg]. Figure 23 shows amount of angle error. A decreasing phenomena of error due to installation angle error compensation is confirmed as in the other results. It can be seen that the error after angle offset compensation is within the allowable range. Figure 22 and 23 show that the posture compensation is also successful. However, it can be seen Figure 23 that the error without compensation is so small that compensation is not necessary in this case, so that no significant effect of compensation is seen in case of $\phi_B$.

**Figure 23** Needle posture error when rotating hand of Zerobot around $\phi_B$ direction with an installation angle offset of –10.08 degree (see online version for colours)

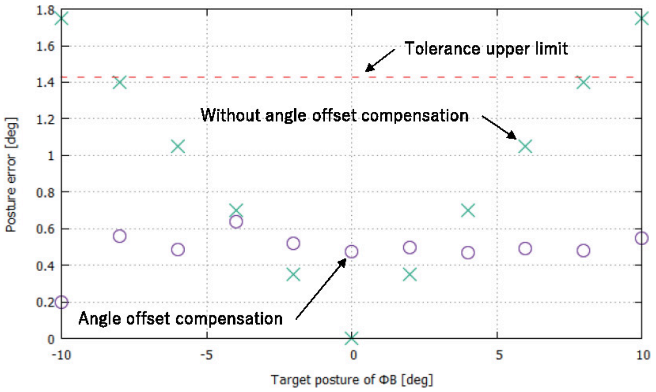


## 7 Conclusion

We have developed Zerobot, an interventional radiology support robot, to eliminate doctor exposure. Zerobot aims to conduct whole process from positioning robot to inserting a needle by remote-control. Risk management of Zerobot was conducted for clinical trial in previous research. These are confirmed that Zerobot can be operated a needle as correctly as the doctor hands and a needle can be punctured into living tissue with Zerobot. In addition, the safety of Zerobot is confirmed by a lot of nonclinical studies which a part of risk management. But Zerobot has two problems that taking long time and increasing patient exposure to accurately puncture. Since, registration is not conducted, these problems are occurred. Therefore, we are proposed automated registration and targeting function in previous research. needle operation time and patient exposure are decreased by using automated registration and targeting function. However, the installation angle offset of the robot was not considered when using automatically registration and targeting function. Therefore, a method to compensation of installation angle offset using CT equipment is proposed. The installation angle offset compensation is successful on all axis.

## Acknowledgement

This work was supported by MEXT KAKENHI Grant Number 17K10439 and Research on Development of New Medical Devices 15652923 from Japan Agency for Medical Research and Development, AMED.

This study was conducted with the help of Dr. Jun Sakurai, Mr. Kazushi Kimura and Prof. Mamoru Minami in Okayama University.

## References

Craig, J.J. (1989) *Introduction to ROBOTICS – Mechanics and Control*, Addison-Wesley, New York.

Hiraki, T., Kamegawa, T., Matsuno, T. and Kanazawa, S. (2014) 'Development of a robot for CT fluoroscopy-guided intervention: free physicians from radiation', *The Official Journal of the Japanese Society of Interventional Radiology*, Vol. 20, No.4, pp.375-381.

Hiraki, T., Kamegawa, T., Matsuno, T., Sakurai, J., Kirita, Y., Matsuura, R., Yamaguchi, T., Sasaki, T., Mitsuhashi, T., Komaki, T., Masaoka, Y., Matsui, Y., Fujiwara, H., Iguchi, T., Gobara, H. and Kanazawa, S. (2017) 'Robotically driven CT-guided needle insertion: preliminary results in phantom and animal experiments', *Radiology*, Vol. 285, No. 2, pp.454–461.

Koethe, Y., Xu, S., Velusamy, G., Wood, B.J. and Venkatesan, A.M. (2013) 'Accuracy and efficacy of percutaneous biopsy and ablation using robotic assistance under computed tomography guidance: a phantom study', *European Radiology*, Vol. 24, No. 3, pp.723–730.

Maurin, B., Bayle, B., Piccin, O., Gangloff, J., de Mathelin, M., Doignon, C., Zanne, P. and Gangi, A. (2008) 'A patient-mounted robotic platform for CT-scan guided procedures', *IEEE Transaction on Biomedical Engineering*, Vol. 55, No. 10, pp.2417–2425.

Monkawa, A. (2012) 'Construction of support system on upstream technology with X-ray computed tomography', *Study Report of Tokyo Metropolitan Industrial Technology Research Institute*, Vol. 7, pp.26–29.

Nakaya, H., Matsuno, T., Kamegawa, T., Hiraki, T., Inoue, T., Yanou, A., Minami, M. and Gofuku, A. (2014) 'CT phantom for development of robotic interventional radiology', *Proc. of IEEE/SICE International Symposium on System Integration (SII2014)*, Tokyo, Japan.

Staianovici, D., Cleary, K., Patriciu, A., Mazilu, D., Stanimir, A., Craciunoiu, N., Watson, V. and Kavoussi, L. (2003) 'AcuBot: a robot for radiological interventions', *IEEE Transaction on Robotics and Automation*, Vol. 19, No. 5, pp.927–930.

Sugiyama, K., Matsuno, T., Kamegawa, T., Hiraki, T., Nakaya, H., Yanou, A. and Minami, M. (2015) 'Reaction force analysis of puncture robot for CT-guided interventional radiology in animal experiment', *Proc. of IEEE/SICE International Symposium on System Integration (SII2015)*, Nagoya, Japan.